EXPERIMENTAL STATUS OF THE STANDARD MODEL

DEAN KARLEN

Ottawa-Carleton Institute for Physics, Carleton University, 1125 Colonel By Drive, Ottawa, CANADA K1S 5B6
E-mail: karlen@physics.carleton.ca

A summary of recent measurements that test the Standard Model of particle physics is presented. These include updates to precision Z^0 measurements by the four LEP experiments and by SLD, electron-positron annihilation above the W^+W^- threshold at LEP II, W production at the Tevatron, neutrino-nucleon scattering measurements from the NuTeV experiment, and early results on low energy hadron production at BES and the anomalous magnetic moment of the muon at BNL E821. All of the measurements reported are in agreement with the Standard Model. These data are used to place constraints on the remaining unknown parameter of the Standard Model, the mass of the Higgs Boson.

1 Introduction

This talk reports on the most recent and precise tests of the Standard Model of electroweak interactions [1] using data from the four LEP experiments, ALEPH, DELPHI, L3 and OPAL, the SLD experiment at SLC, the Tevatron experiments, CDF and D0, the NuTeV neutrino-nucleon scattering experiment. Early measurements of the electron-positron cross section near the charm threshold by BES and of the muon anomalous magnetic moment by the BNL experiment E821, which will contribute to future precision tests of the Standard Model are also presented.

After a report on the recent performance of the currently active high energy colliders, the experimental results will be summarized as follows. In section 2, the measurements specific to W properties are discussed, followed by a summary of recent Z^0 measurements, in section 3. Other Standard Model measurements are reported on in section 4. Finally, the interpretation of the precision data in the Standard Model framework is given in section 5.

1.1 LEP and SLC performance

The LEP II programme is well underway, with LEP providing significant luminosity at ever increasing energies each year as shown in Figure 1. The data recorded since the beginning of 1997 results in much improved measurements of W properties from LEP, as compared to results that were presented at the summer conferences a year ago. It is reasonable to expect that the goal of 500 pb^{-1} delivered to each experiment at energies above the W^+W^- threshold will be achieved before the scheduled completion of the LEP programme in the year 2000.

The SLC has just completed a very successful run over the past 10 months, as demonstrated in Figure 2. High luminosity and high polarisation during this run has resulted in a much improved measurement of the weak mixing angle. The SLD experiment is requesting that they have an additional run in the future, to improve this measurement further.

1.2 LEP and SLC beam energy calibration

Detailed evaluation of the LEP beam energies and uncertainties for the Z^0 running though 1995 is now complete.[2] The contribution to the uncertainties in the Z^0 mass and width are approximately 1.5 MeV.[3] At LEP II, the beam energy is much less precisely determined, due to the large extrapolation from the highest beam energies in which the resonant depolarisation technique may be applied (roughly 55 GeV) to current beam energies (above 90 GeV).[4] The uncertainty in the beam energies in the 1997 data is approximately 25 MeV, leading to a contribution to the W mass uncertainty of 20 MeV. A method to cross check the beam energy measurement, using radiative return events, has been performed by the ALEPH experiment with their 1997 data.[4,5] The beam energy measured in this way would contribute an uncertainty in the W mass of 102 MeV, which is still smaller than their remaining experimental error of 139 MeV. A project to install a precise spectrometer in LEP is underway with a goal to attain a precision of 10 MeV beginning in 1999.[4]

The SLC beam energy calibration was checked using a short 3-point scan of the Z^0 resonance,[6] and indicated a error of 49 ± 22 MeV in the determination of the centre of mass energy. As a result, a correction is applied to the SLD measurement of weak mixing angle, but the correction is only about one third of the overall uncertainty in the measurement.

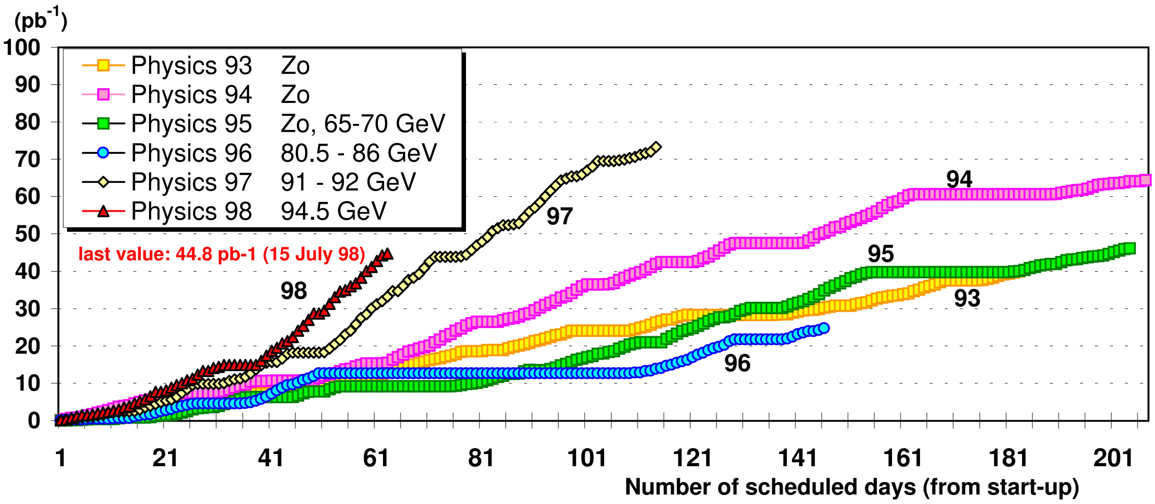

Figure 1: The integrated luminosity seen by the LEP experiments from 1993 through July 15, 1998. The LEP-2 design goal of delivering 500 pb^{-1} above the W^+W^- threshold to each experiment is within reach.

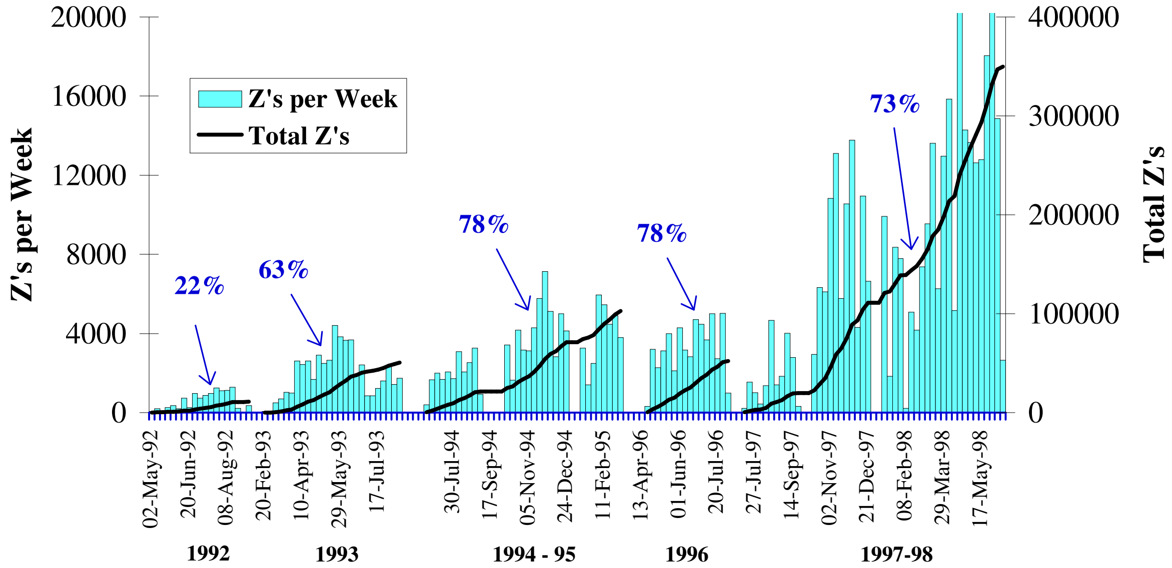

Figure 2: The number of Z^0 events collected by the SLD experiment each week (histogram) and integrated over each running period (line) is shown for the period between May 1992 and May 1998. A significant improvement in the performance of SLC is seen in the running period just completed. The average polarisations for each running period is indicated.

Table 1: The branching ratios for the W pair decay modes (BR) and typical purities (Π) and efficiencies (ϵ) for their selection by the LEP experiments.

	BR (%)	Π (%)	ϵ (%)
$W^+W^- \to q\bar{q}'q\bar{q}'$	46	80	85
$W^+W^- \to q\bar{q}'\ell\nu_\ell$	44	90	80
$W^+W^- \to \ell^+\nu_\ell\ell^-\bar{\nu}_\ell$	10	90	70

2 W properties

2.1 W mass measurements

The mass of the W is measured at the Tevatron by fitting the $\ell^\pm\nu$ transverse mass distributions.[7] The D0 experiment also fits the electron p_t distribution. The results from the two experiments are:

$$\begin{array}{ll} \text{CDF (prelim.)} & m_W = 80.38 \pm 0.12 \text{ GeV} \\ \text{D0} & m_W = 80.43 \pm 0.11 \text{ GeV} \end{array}$$

At LEP, W's are most often produced in pairs, and all decay channels are selected with high efficiency and purity, as shown in Table 1. The experiments employ various multivariate techniques to optimise the signal and purity of the event selections.

The W mass is estimated from direct reconstruction of jet-jet invariant masses in these events with kinematic fitting applied to improve the mass resolution.[8] The four quark final state has the complication of three possible jet pairings, amongst the four jets. The kinematic fit χ^2, jet charge, and/or angles are used to help determine the correct combination.

An additional complication in the fully hadronic channel arises from the fact that the decays of the two W's are not independent. Since the W decay length is much smaller than the hadronization scale, the interconnection of decays may affect the estimation of the W mass in this channel.

Two effects of this type are Bose-Einstein correlations and colour reconnection. Bose-Einstein correlations, an enhancement of identical bosons produced nearby in phase space, has been observed in Z^0 decays, but it is not understood if the same effect exists between pions arising from different W bosons. Colour reconnection could result in a significant interference effect in the hadronization process, but one has to rely on models to estimate its magnitude. These models generally predict a slight reduction in multiplicity, possibly enhanced at low momentum and for heavy hadrons.

So far, there is no experimental evidence for significant interconnection effects in fully hadronic W^+W^- decays.[9,10] No additional enhancement at low Q, where $Q = |p_1 - p_2|$ and p_i is the four momentum of same sign pions, which would be expected if strong Bose-Einstein correlations existed between different W bosons. The maximum bias in the W mass measurement, with full Bose-Einstein correlations, is estimated to be -50 MeV. Likewise, a reduction in charged particle multiplicity, that could indicate significant colour reconnection, is unobserved. The LEP experiments currently assign a 90 MeV systematic uncertainty to the W mass measurement in the fully hadronic mode for interconnection effects.

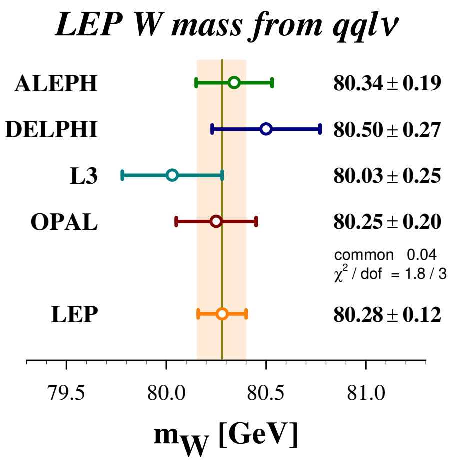

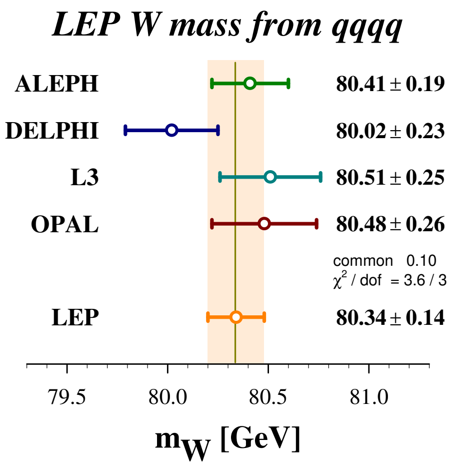

Figure 3: W mass measurements from LEP from the semi-leptonic and fully hadronic decay channels. The fully hadronic channel has a larger common systematic uncertainty assigned, due to possible interconnection effects.

The measurements of the W mass from the data collected at 183 GeV (in 1997) is shown in Figure 3.[12,8] When combined with earlier LEP II measurements, the result is

$$\text{LEP}: \quad m_W = 80.37 \pm 0.09 \text{ GeV}$$

in good agreement with the Tevatron results.

2.2 W width

The most precise, but indirect, estimate of the W width is found from the relation,

$$\frac{\sigma_{\rm W}\cdot {\rm BR}({\rm W}\to \ell\nu)}{\sigma_{\rm Z}\cdot {\rm BR}({\rm Z}\to \ell\ell)} = \frac{\sigma_{\rm W}\cdot \Gamma({\rm W}\to \ell\nu)\,\Gamma_{\rm Z}}{\sigma_{\rm Z}\cdot \Gamma({\rm Z}\to \ell\ell)\,\Gamma_{\rm W}} \qquad (1)$$

by using W production data from hadron colliders, Z^0 data from LEP, and the Standard Model estimate for BR(W→ $\ell\nu$). The width found this way is,[7]

$$\Gamma_{\rm W} = 2.06 \pm 0.06 \quad {\rm GeV}\ .$$

The CDF experiment makes a less model dependent determination of

$$\Gamma_{\rm W} = 2.19 \pm 0.17 \pm 0.09 \quad {\rm GeV} \quad \text{(preliminary)}$$

by fitting the tail of the transverse mass distribution.[11] The LEP experiments can directly fit the mass distribution of the W candidates, and the following preliminary results are found,[12]

$$\Gamma_{\rm W} = 2.41 \pm 0.39 \pm 0.25 \quad {\rm GeV} \quad \text{(L3)}$$
$$\Gamma_{\rm W} = 2.25 \pm 0.37 \pm 0.17 \quad {\rm GeV} \quad \text{(OPAL).}$$

All of these measurements are consistent with the Standard Model expectation of 2.077 ± 0.014 GeV.

2.3 W branching ratios, lepton universality, and V_{cs}

The W leptonic and hadronic branching ratios as measured by the LEP experiments are summarized in Figure 4. The D0 experiment measures ratios of leptonic branching ratios to be,[7]

$$\frac{{\rm BR}({\rm W}\to \tau\nu)}{{\rm BR}({\rm W}\to e\nu)} = 1.00 \pm 0.06$$
$$\frac{{\rm BR}({\rm W}\to \mu\nu)}{{\rm BR}({\rm W}\to e\nu)} = 1.00 \pm 0.08\ .$$

All of the W branching ratio measurements support lepton universality in charged current interactions, but less precisely than measurements from τ decays. By comparing the τ and μ lifetimes, and accounting for the difference in their masses and electronic branching ratios, the ratio of the τ and μ weak coupling constants is found to be,[13]

$$g_\tau/g_\mu = 1.0001 \pm 0.0026$$

and the agreement with measurements and universality is demonstrated in Figure 5. By comparing the ratio of electronic and muonic branching ratios, the ratio of the μ and e weak coupling constants is found to be,[13]

$$g_\mu/g_e = 1.0015 \pm 0.0025\ .$$

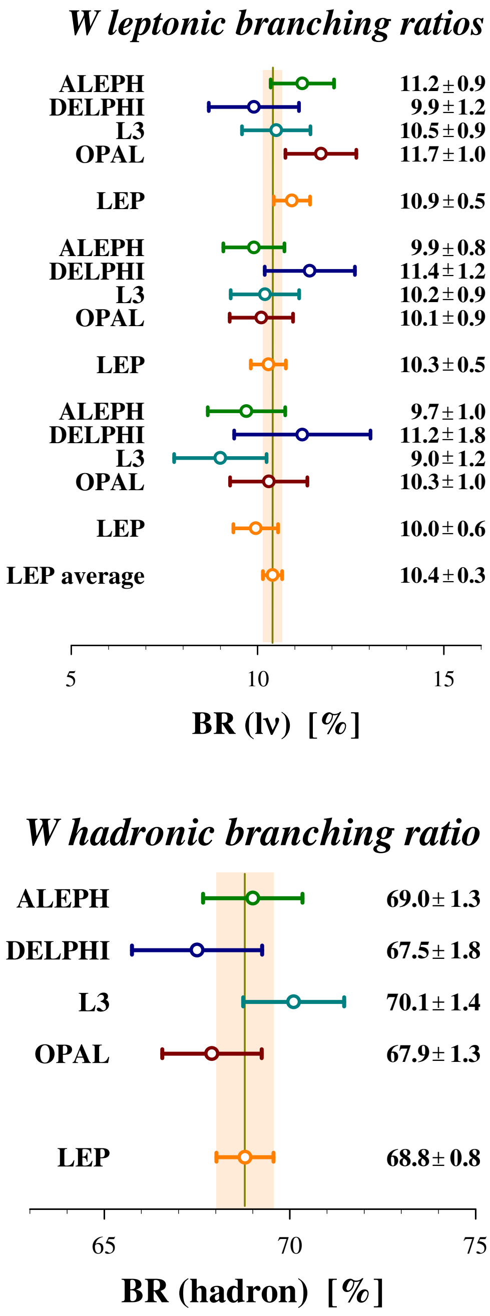

Figure 4: W branching ratio measurements from the LEP experiments.

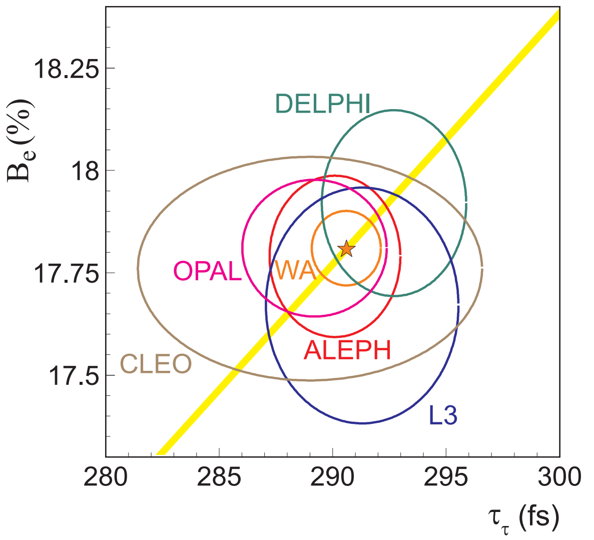

Figure 5: Comparison of the τ electronic branching ratio and its measured lifetime from the LEP experiments and CLEO (one sigma confidence contours), with the expectation assuming lepton universality (diagonal line). The star and the immediately surrounding ellipse (labeled WA) is the world average combination of the measurements shown.

The W hadronic branching ratio, as measured at LEP,[15]

$$B_h \equiv BR(W \to \text{hadrons}) = 0.6879 \pm 0.0077$$

can be related to the CKM matrix elements by,

$$\frac{B_h}{1 - B_h} = \sum_{i=u,c} \sum_{j=d,s,b} |V_{ij}|^2 \left(1 + \frac{\alpha_s}{\pi}\right) \quad .$$

Since V_{cs} is the least well known, it is useful to use this relation to estimate V_{cs}, which gives the result

$$|V_{cs}| = 1.04 \pm 0.04 \quad \text{(LEP indirect average)}.$$

The LEP experiments also measure this directly by tagging charm in W decays giving,[16]

$$|V_{cs}| = 0.99 \pm 0.11 \quad \text{(LEP direct average)}.$$

2.4 W production measurements

The D0 experiment has new (preliminary) results,[7]

$$\sigma_W \cdot BR(W \to e\nu) = 2.38 \pm 0.01 \pm 0.09 \pm 0.20 \quad \text{nb}$$
$$\sigma_W \cdot BR(W \to \mu\nu) = 2.38 \pm 0.03 \pm 0.17 \pm 0.13 \quad \text{nb}$$

consistent with expectations. The HERA experiments also observe W production by identifying leptons with high transverse momenta.[14] The results are shown in Table 2, where it is seen that the H1 experiment observes an excess in the muon channel.

Table 2: W production at HERA.

	W→ $e\nu$ selection		
	obs.	W→ $e\nu$	bckgnd
ZEUS	3	2.0	1 ± 0.5
H1	1	1.7	0.7
	W→ $\mu\nu$ selection		
	obs.	W→ $\mu\nu$	bckgnd
ZEUS	0	0.6	0.6 ± 0.2
H1	5	0.5	0.3

Table 3: Measurements of single W production at LEP. The number of candidates (N_{obs}) in the lepton decay mode is shown along with the total expected number and the expected number of signal events.

	E_{cm} (GeV)	$\mathcal{L}$ (pb^{-1})	N_{obs}	N_{exp}	$N_{e\nu\text{W}}$
ALEPH	161-183	78.9	11	11.1	7.3
DELPHI	161-183	73.0	9	5.4	5.2
L3	130-183	88.5	12	10.2	6.0
OPAL	161-172	20.3	2	2.0	0.8

To compare the W pair production rate at LEP with theory, each experiment corrects their observed rates to that corresponding to the CC03 diagrams. These three diagrams, photon and Z^0 in s-channel and neutrino exchange, represent the dominant amplitudes. As shown in Figure 6, the experiments are in good agreement with each other for both 183 GeV data (1997) and 189 GeV data (1998).[15] The 189 GeV data is somewhat lower than the expectations, but is inconsistent with removal of specific amplitudes as shown in Figure 7. There is no need to speculate about an anomalous W pair cross section at 189 GeV at this time, since the precision of the measurement will improve by about a factor of two before the end of 1998.

2.5 Single W production

The LEP experiments also measure single W production, for both hadronic and leptonic decay modes. In Table 3, the results of the measurements in the cleaner leptonic modes are shown.[17]

ALEPH uses their observed single W cross section to determine the partial width of the W into invisible or nearly invisible final states.[17] Decays with little visible energy could result, for example, from modes involving supersymmetric particles where there are nearly degenerate sparticles in the decay chain. Their analysis selects single W events consistent with W pair events, but where only one W is seen. No excess is seen in this channel and,

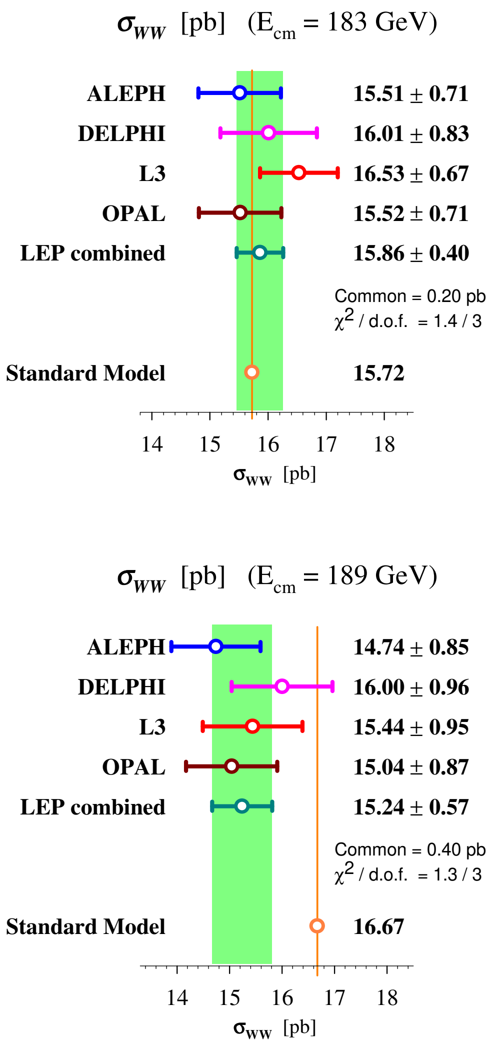

Figure 6: W pair cross sections as measured by the LEP experiments for the 183 GeV and 189 GeV data.

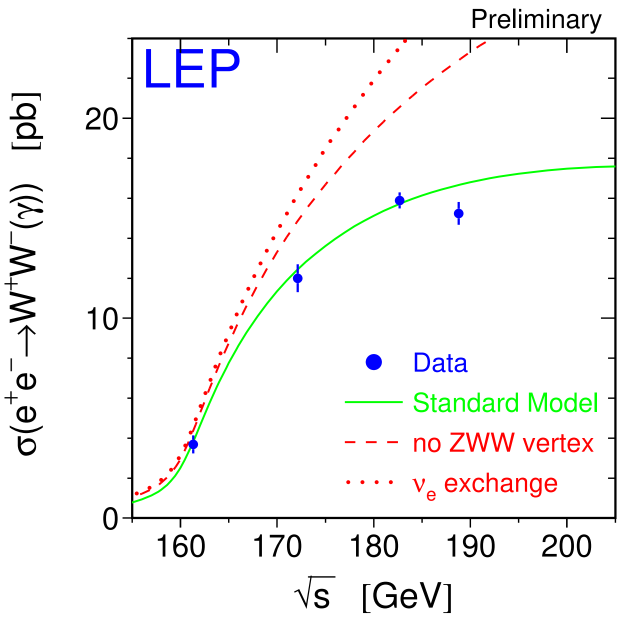

Figure 7: LEP combined W pair cross sections as a function of centre-of-mass energy. The s-channel (triple gauge coupling) amplitudes are significant at energies above 180 GeV.

as a result, a limit is placed on the (nearly) invisible partial width,

$$\Gamma_{\mathrm{W}}(\mathrm{inv}) < 27 \ \ \mathrm{MeV\ at}\ 95\%\ \mathrm{C.L.}$$

This is an improvement over other methods that limit the invisible W width. The indirect width (equation 1) gives a limit of 109 MeV [7] and the W pair cross section dependence on the W width gives 41 MeV.[15]

2.6 Triple gauge couplings

An important aspect of the Standard Model of electroweak interactions, that is just beginning to be confronted with precision measurements, is the self couplings of the gauge bosons. To perform a quantitative search for anomalous couplings, one can consider the most general Lorentz invariant Lagrangian describing WWZ and WWγ interactions. This results, however, in 14 terms, each with its own coupling constant.[18] To reduce the parameter space, physics insight is used to suggest the most interesting combinations of terms, that is, those that are not already strongly excluded. Three couplings remain, labeled $\Delta\kappa_\gamma$, Δg_1^z, and λ, all of which are zero in the Standard Model. These parameters are related to the static moments of the W^+ by,

$$\begin{array}{ll} \text{magnetic dipole:} & \mu_{\mathrm{W}} = (e/2m_{\mathrm{W}})(2 + \Delta\kappa_\gamma + \lambda) \\ \text{electric dipole:} & q_{\mathrm{W}} = -(e/2m_{\mathrm{W}}^2)(1 + \Delta\kappa_\gamma - \lambda) \ . \end{array}$$

LEP experiments are sensitive to anomalous triple gauge couplings through the W pair cross section, the angular distribution of the produced W's, and their helicity components, which are deduced from the angles of the W decay products. In addition, single W and single γ production is also sensitive to the WWγ vertex.

At the Tevatron, the D0 experiment investigates anomalous triple gauge couplings by measuring gauge boson pair production cross sections in the following channels,[19]

$$\begin{array}{ll|ll|ll} \mathrm{W} & \gamma & \mathrm{W} & \mathrm{W} & \mathrm{W} & (\mathrm{W/Z}) \\ \hookrightarrow \ell\nu & & \hookrightarrow \ell\nu & \hookrightarrow \ell\nu & \hookrightarrow e\nu & \hookrightarrow \mathrm{qq} \end{array} .$$

The enhancement of the gauge boson pair cross section from anomalous couplings increases with s, which in principle gives an advantage to Tevatron experiments compared with LEP. However, since the backgrounds are larger at the Tevatron, the overall sensitivity is similar to that of the LEP experiments, as shown in Figure 8. The combined measurements of the anomalous couplings are,[18]

$$\begin{aligned} \Delta\kappa_\gamma &= 0.13 \pm 0.14 \\ \Delta g_1^Z &= 0.00 \pm 0.08 \\ \lambda_\gamma &= -0.03 \pm 0.07 \end{aligned}$$

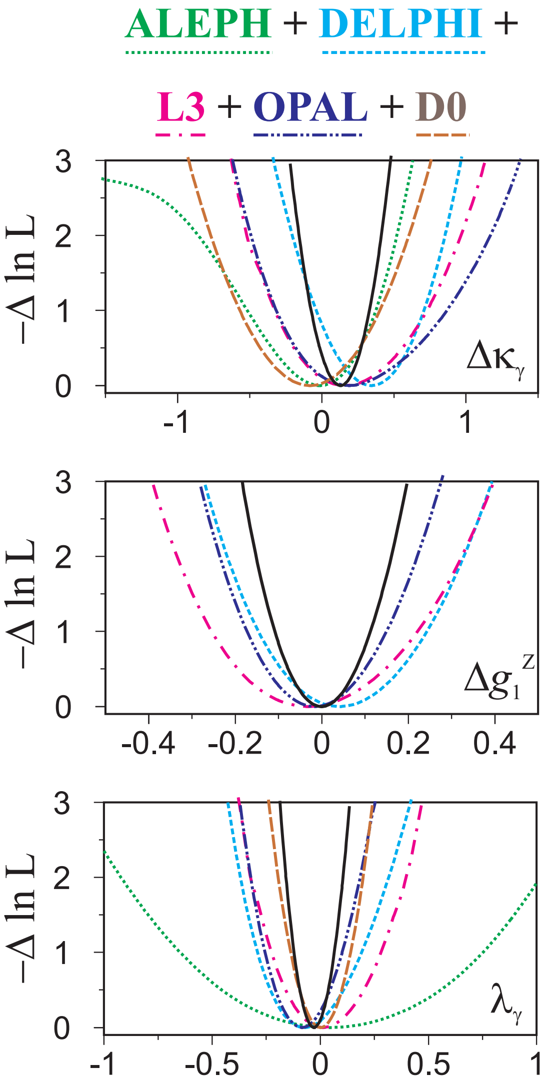

Figure 8: Log-likelihood curves for the determinations of anomalous coupling constants from D0 and each of the LEP experiments (various dashed lines). The combination of these results is shown by the solid curve.

3 Z^0 properties

In the past year the SLD experiment at SLC significantly increased their data sample with high beam polarisation and there have been further refinements in the analyses of the data collected by the LEP experiments near the Z^0 peak, during the period 1990-1995.

3.1 Z^0 lineshape and forward-backward asymmetries

The LEP experiments average their results by using a common set of nine relatively uncorrelated lineshape and asymmetry parameters.[3,20,21] With measurements on and off the peak, the experiments fit the e^+e^- excitation curve for the mass and width of the Z^0 boson, m_Z and Γ_Z, and the pole hadronic cross section, σ^0_{had}, by using a Breit-Wigner resonance, with an s-dependent width. The remaining parameters are the three ratios of hadronic to leptonic partial widths, $R_\ell = \Gamma_{\mathrm{had}}/\Gamma_\ell$, and the three leptonic pole asymmetries, $A^{0,\ell}_{\mathrm{FB}}$.

The parameters are corrected for initial state radiation and, for the e^+e^- final states, the contribution from the t-channel amplitude. Recently, order α^3 corrections have been included,[22,23,24] which modify the mass, width and pole cross section. Since these corrections are still under study, the systematic errors on these quantities have been inflated to account for the small changes, rather than changing the central values.

The leptonic forward-backward asymmetries and partial widths are shown in Figure 9. Assuming lepton universality, the combined LEP results are,

$$\begin{aligned} m_Z &= 91186.7 \pm 2.1 \;\; \mathrm{MeV} \\ \Gamma_Z &= 2493.9 \pm 2.4 \;\; \mathrm{MeV} \\ \sigma^0_{\mathrm{had}} &= 41.491 \pm 0.058 \;\; \mathrm{nb} \\ R_\ell &= 20.765 \pm 0.026 \\ A^{0,\ell}_{\mathrm{FB}} &= 0.01683 \pm 0.00096 \;\; . \end{aligned}$$

The hadronic and leptonic widths are found to be

$$\begin{aligned} \Gamma_{\mathrm{had}} &= 1742.3 \pm 2.3 \;\; \mathrm{MeV} \\ \Gamma_\ell &= 83.90 \pm 0.10 \;\; \mathrm{MeV} \end{aligned}$$

which can be used to determine the invisible width:

$$\begin{aligned} \Gamma_{\mathrm{inv}} &= \Gamma_Z - \Gamma_{\mathrm{had}} - (3 + \Delta_\tau)\Gamma_\ell \\ &= 500.1 \pm 1.9 \;\; \mathrm{MeV} \; . \end{aligned}$$

Using the Standard Model ratio of charged lepton and neutrino partial widths, the result corresponds to the number of neutrino generations of

$$N_\nu = 2.994 \pm 0.011 \; .$$

At the 95% confidence level, additional contributions to the Z^0 invisible width are limited to 2.8 MeV. These invisible width measurements are limited by the current 0.11% theoretical uncertainties in the luminosity measurement, which are expected to reduce to 0.06%.[25]

3.2 Polarisation asymmetries

With its ability to produce e^- beams with large longitudinal polarisation, the SLC enables the SLD experiment to measure the left-right polarisation asymmetry, A_{LR}. The precision of A_{LR} has improved with the inclusion of the recent data and two new polarimeters have confirmed the critical polarisation measurements made by the Compton polarimeter. The preliminary result from the complete SLD data sample is,[26]

$$A_{\mathrm{LR}} = A_e = 0.1510 \pm 0.0025 \;\; .$$

New preliminary results from ALEPH and DELPHI dramatically improve the precision of the LEP combined measurements of τ polarisation.[27] The results, in terms of the leptonic coupling parameters, are

$$A_e = 0.1479 \pm 0.0051 \qquad A_\tau = 0.1431 \pm 0.0045 \;\; .$$

The leptonic coupling constants derived from the polarisation asymmetries and the forward backward asymmetries can be combined with the partial widths to estimate the effective vector and axial vector coupling constants, $g_{V\ell}$ and $g_{A\ell}$. The resulting contours are shown in Figure 10. Assuming lepton universality, the combined LEP and SLD measurements of the effective coupling constants are,

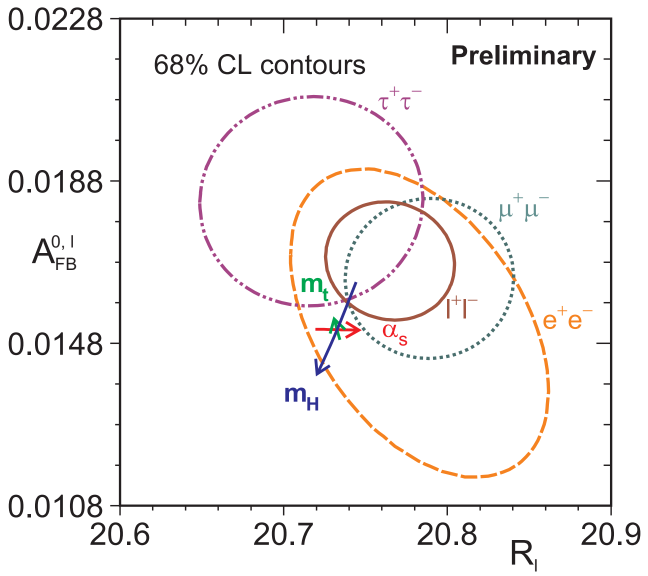

Figure 9: The LEP combined measurements of the leptonic forward-backward asymmetries and partial widths are shown. The solid contour shows the result from the assumption of lepton universality. The Standard Model expectation is shown for the parameters, $\alpha_s(m_Z^2) = 0.119 \pm 0.002$, $m_t = 173.8 \pm 5.0$ GeV, and $m_H = 300^{+700}_{-210}$ GeV, where the arrows point in the direction of increasing these parameters.

$$\begin{aligned} g_{V\ell} &= -0.03753 \pm 0.00044 \\ g_{A\ell} &= -0.50102 \pm 0.00030 \end{aligned}$$

3.3 Heavy flavour results

The electroweak couplings for charm and bottom quarks are determined by measuring their production rates,[28] their forward-backward asymmetries,[29] and, in the case of SLD, their left-right forward-backward asymmetries.[30] The heavy quarks and their charges are identified by lifetime, event shape, lepton, and D-meson tagging. Since many of the techniques are common amongst the experiments, a complex averaging scheme has been developed that properly takes into account the correlated systematics.[31] The production rate of charm and bottom quarks in Z^0 decay, expressed as a fraction of all hadronic decays, is shown in Figure 11. The combined LEP and SLD measurements are:

$$\begin{aligned} R_b &= 0.21656 \pm 0.00074 \\ R_c &= 0.1735 \pm 0.0044 \\ A^{0,b}_{\mathrm{FB}} &= 0.0990 \pm 0.0021 \\ A^{0,c}_{\mathrm{FB}} &= 0.0709 \pm 0.0044 \end{aligned}$$

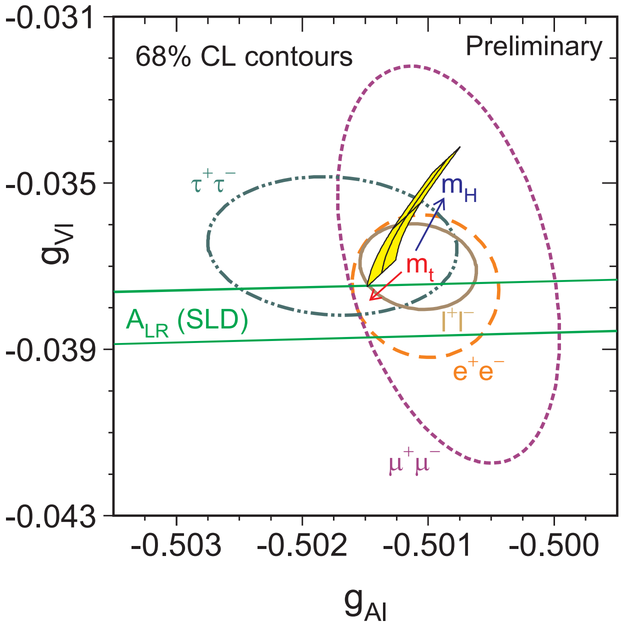

Figure 10: The LEP combined measurements of the leptonic effective vector and axial vector coupling constants are shown. The solid contour shows the result from the assumption of lepton universality, and the band represents the result from the SLD measurement of the left-right polarisation asymmetry. The Standard Model expectation is shown for the parameters, $m_t = 173.8 \pm 5.0$ GeV, and $m_H = 300^{+700}_{-210}$ GeV, where the arrows point in the direction of increasing these parameters.

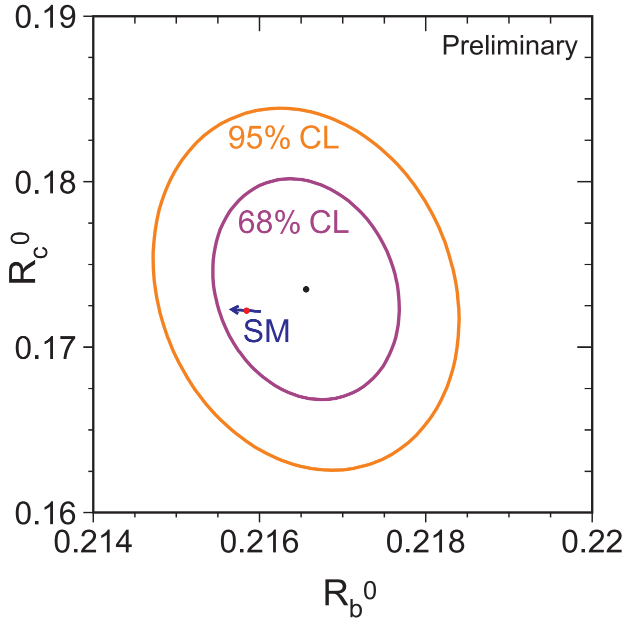

Figure 11: The ratios of the heavy flavour partial widths of the Z^0 to its total hadronic partial widths is shown for the combined LEP and SLD measurements. The Standard Model expectation is shown for the parameter, $m_t = 173.8 \pm 5.0$ GeV, where the arrows point in the direction of increasing top mass.

$$
\begin{aligned}
A_b &= 0.867 \pm 0.035 \\
A_c &= 0.647 \pm 0.040 \quad .
\end{aligned}
$$

3.4 Effective electroweak mixing angle

The various asymmetry measurements from LEP and SLD can each be expressed as a measurement of the effective electroweak mixing angle, $\sin^2\theta_{\rm eff}^{\rm lept}$, which is defined in terms of the effective vector and axial vector coupling constants as,

$$
\sin^2\theta_{\rm eff}^{\rm lept} \equiv \frac{1}{4}\left(1 - \frac{g_{V\ell}}{g_{A\ell}}\right) \quad .
$$

Figure 12 compares the measurements,[21] and it is seen that the two most precise ones, the left-right asymmetry from SLD and the bottom quark forward backward asymmetry, differ by 2.4 σ. Overall, however, there is relatively good agreement amongst the measurements, with χ^2 of 7.8 for 6 degrees of freedom.

3.5 Fermion pair production above the Z^0

Unlike for data samples collected at the Z^0 peak, fermion pair production at higher energies is often accompanied

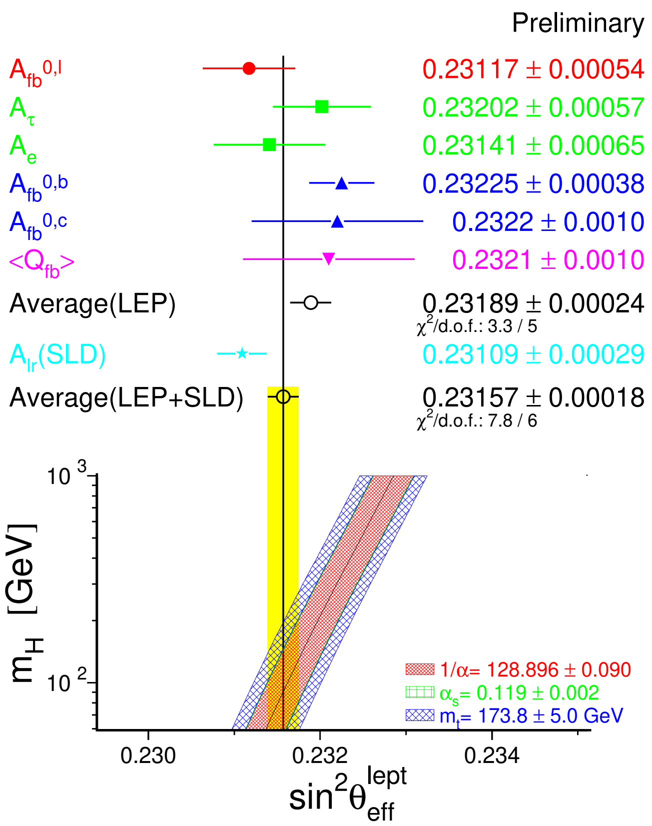

Figure 12: Asymmetry measurements expressed in terms of the effective electroweak mixing angle. Also shown is the Standard Model prediction as a function of the Higgs mass.

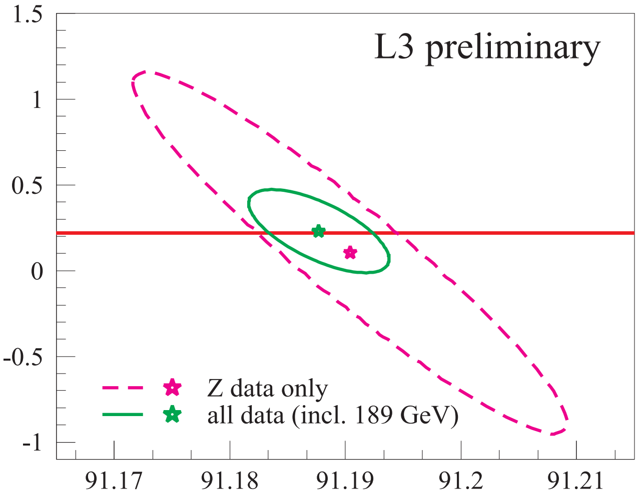

Figure 13: The results from an S-matrix fit to L3 data at the Z^0 peak is shown by the dashed contour. When higher energy data is included, the interference term is much better determined, thus reducing the Z^0 mass uncertainty.

by significant initial state radiation. This initial state radiation typically brings the effective centre-of-mass energy back to the Z^0 peak energy, so it is important to remove events of this type from consideration. The LEP experiments calculate the effective centre-of-mass energy from kinematic fits (for hadrons) and acollinearity angles (for leptons), and remove those events with more than about 15% reduction of the centre-of-mass energy. Combined results of the LEP experiments are not performed, since different requirements are made for each experiment. Each experiment finds good agreement with Standard Model expectations for the production rates and asymmetries.[32,33]

Measurements of fermion pair production above the Z^0 peak provide a test of the γ-Z^0 interference terms. The standard electroweak fits, discussed in Section 5, fix the γ-Z^0 interference term to the Standard Model value, since the data at the peak does not constrain it well. An alternative approach, the S-matrix fit, includes variable scale factors for the interference terms. In the S-matrix fit, there is a large correlation between the Z^0 mass and the hadronic γ-Z^0 interference term, $j^{\rm tot}_{\rm had}$, which therefore inflates the Z^0 mass uncertainty. The effect is much reduced when fermion pair production above the Z^0 peak is included in the S-matrix fit, as demonstrated in Figure 13.[32]

4 Other SM processes

4.1 LEP measurements

Each increase in the LEP centre-of-mass energy brings the possibility that the measurement of some well understood process will begin to diverge from the Standard Model prediction. Examples of angular distributions from such processes are shown in Figure 14. The LEP measurements of the two-photon annihilation process show no evidence for new physics.[34] Limits can be placed on various new contact terms in the range 300 to 1300 GeV, and on the mass of an exchanged excited electron, of about 280 GeV. Electron scattering with a nearly real photon radiated by another electron is also in good agreement with expectations for both the $e\gamma$ and the $e\,Z^0/\gamma^*$ (with $Z^0/\gamma^* \to$ hadrons) final states.[35]

Last year LEP crossed the threshold for Z^0 pair production. Cross section measurements from 183 GeV and 189 GeV data are in good agreement with expectations, albeit with very large statistical errors.[35]

4.2 Neutrino-nucleon scattering

The ratio of neutral current and charged current cross sections for neutrino nucleon scattering is sensitive to the electroweak mixing angle. By using a ν_μ beam, the CCFR experiment determined the on-shell value to be $\sin^2\theta_{\rm W} = 0.2236 \pm 0.0041$.[36] The largest systematic uncertainty came from the calculation of charged current charm production from scattering off sea quarks. The uncertainty in the ν_e contamination of the beam was another large source of error.

The NuTeV experiment was designed to overcome these limiting systematics by measuring the quantity,

$$R^- = \frac{\sigma^{\nu}_{\rm NC} - \sigma^{\bar\nu}_{\rm NC}}{\sigma^{\nu}_{\rm CC} - \sigma^{\bar\nu}_{\rm CC}}$$

in which the effect of scattering off sea quarks cancel, and by using a modified beam line which reduces the ν_e contamination.[36] Charged current events are distinguished from neutral current events by the presence of a highly penetrating track (muon), which results in a large spatial extent of the event. The preliminary result from NuTeV using their complete data sample is,

$$\sin^2\theta_{\rm W}^{\rm on-shell} = 0.2253 \pm 0.0019 \pm 0.0010$$

where the first error is statistical and the second systematic. This is twice as precise as the best previous measurement from neutrino nucleon scattering (CCFR).

4.3 Hadronic cross section measurements from BES

The interpretation of precision measurements at the electroweak scale relies on the knowledge of the electromagnetic coupling constant at that scale, $\alpha(m_{\rm Z}^2)$. The largest uncertainty in this quantity arises from the hadronic vacuum polarisation corrections.[37,38] The uncertainty can be reduced by improved measurements of the hadronic cross

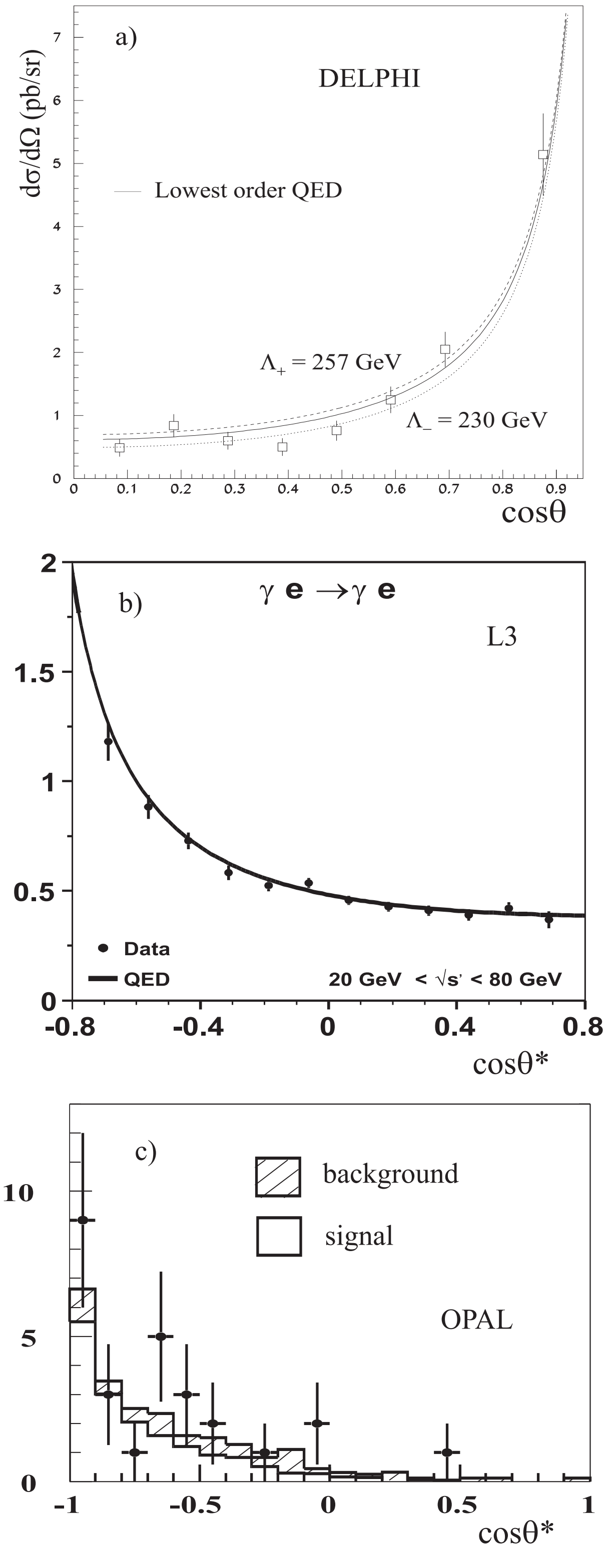

Figure 14: Angular distributions for other standard model processes measured at LEP: a) the process $e^+e^- \to \gamma\gamma(\gamma)$ as measured by DELPHI at $\sqrt{s} = 183$ GeV; b) the process $e^+e^- \to (e)e\gamma$ as measured by L3 at $\sqrt{s} = 172$ GeV; and c) the process $e^+e^- \to (e)eZ^0/\gamma^*$ as measured by OPAL at $\sqrt{s} = 183$ GeV.

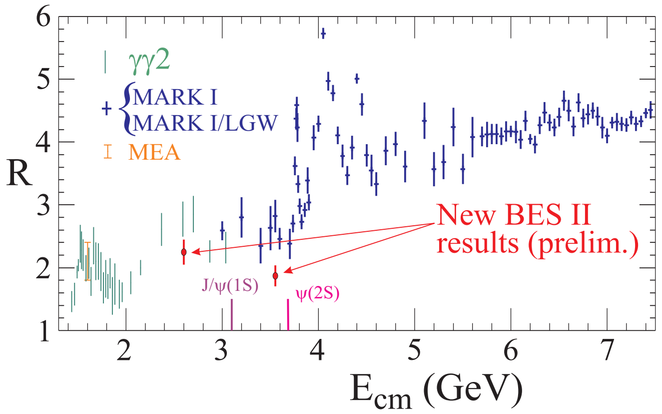

Figure 15: First measurements from the BES experiment of the hadronic cross section at low energies is compared to existing measurements.

section in the range of 2 to 5 GeV. The BES experiment will be performing such a measurement this year, and their first results are shown in Figure 15.

A good understanding of the hadronic vacuum polarization is also important for the measurement of the anomalous magnetic moment of the muon, discussed in the following section.

4.4 BNL experiment E821

The goal of the experiment is to measure the muon anomalous magnetic moment to a precision of about 0.35 parts per million (ppm). This would allow a measurement of the weak contribution, which is 1.3 ppm. The experiment uses a 14 m diameter ring to store muons and precess their spins. Electrons from the muon decay are detected in lead-scintillating-fibre calorimeters. Since the electrons preferentially decay along the muon spin direction, and the muon spin is precessing, the number of electrons observed above a certain energy will oscillate with time. The frequency of the oscillation, the precession frequency of the muon, is proportional to the anomalous magnetic moment, a_μ. The result from the 1997 run is,[39]

$$a_\mu = 1165925(15) \times 10^{-9}$$

which is in good agreement with previous CERN measurements of $a_{\mu^+} = 1165910(11) \times 10^{-9}$ and $a_{\mu^-} = 1165937(12) \times 10^{-9}$. The expected error for the 1998-1999 run is about 1×10^{-9}.

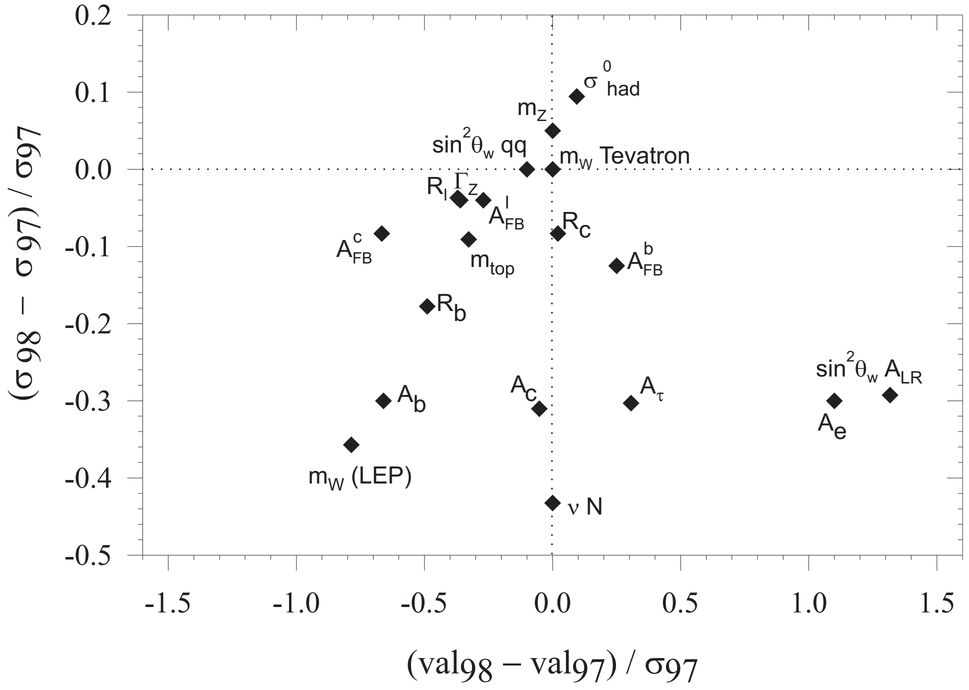

Figure 16: A summary of changes in precision electroweak measurements, used in the global electroweak fit, since the Summer of 1997. The horizontal axis shows the changes in the central values, as a fraction of the 1997 uncertainties. A healthy spread of order 1 σ is observed, for measurements with improved precision. The vertical axis shows the change in uncertainties, relative to the 1997 uncertainties.

Table 4: Results of the global electroweak fits to LEP data alone, to all data except the direct W mass measurements, and to all data. Theoretical errors, due to uncalculated higher order corrections, are not included in the errors.

	LEP alone	all but m_W	all data
m_t (GeV)	160^{+13}_{-9}	171.0 ± 4.9	171.0 ± 4.9
m_H (GeV)	60^{+127}_{-35}	82^{+95}_{-51}	76^{+85}_{-47}
$\alpha_s(m_\mathrm{Z}^2)$	0.121 ± 0.003	0.120 ± 0.003	0.119 ± 0.003
χ^2/d.o.f.	4/9	15/13	15/15
$\sin^2\theta_\mathrm{eff}^\mathrm{lept}$	0.23182 ± 0.00023	0.23159 ± 0.00020	0.23157 ± 0.00019
m_W (GeV)	80.314 ± 0.038	80.367 ± 0.029	80.371 ± 0.026

5 Interpretation of precision data

A global electroweak fit is performed by including as input,[20]

- Z^0 measurements from LEP and SLD
- W mass measurements from LEP II and Tevatron
- $\sin^2\theta_\mathrm{W}$ from the NuTeV and CCFR experiments
- top quark mass from the Tevatron
- $1/\alpha^{(5)}(m_\mathrm{Z}^2) = 128.878 \pm 0.090$,

where $\alpha^{(5)}$ denotes the value calculated without including the top quark contribution.[40,41,21]

There have been a number of measurements whose precision has improved significantly over the past year, as seen in Figure 16. Most notable improvements having impact on the electroweak fit are the new νN scattering result from NuTeV, the W mass determination from LEP data at 183 GeV, the improved precision in the τ polarisation measurements (A_e and A_τ), and the new A_LR measurement from SLD.

The results of the global electroweak fit are shown in Table 4.[20,21] Overall goodness of fit for the three cases shown are all reasonable. The pulls of the individual measurements, for the fit that uses all the data, are summarized in Figure 17.

When all data except m_W is used, the indirect estimate of the W mass has a error of 29 MeV, much smaller than the current uncertainty of the direct W mass measurements, as shown in Figure 18.

The direct measurements of the top quark and W masses are compared with the indirect determination

	Measurement	Pull
m_Z (GeV)	91.1867 ± 0.0021	.09
Γ_Z (GeV)	2.4939 ± 0.0024	-.80
σ^0_{hadr} (nb)	41.491 ± 0.058	.31
R_e	20.765 ± 0.026	.66
$A_{fb}^{0,e}$	0.01683 ± 0.00096	.73
A_e	0.1479 ± 0.0051	.25
A_τ	0.1431 ± 0.0045	-.79
$\sin^2\theta_{eff}^{LEPT}$	0.2321 ± 0.0010	.53
m_W (GeV)	80.37 ± 0.09	-.01
R_b	0.21656 ± 0.00074	.90
R_c	0.1735 ± 0.0044	.29
$A_{fb}^{0,b}$	0.0990 ± 0.0021	-1.81
$A_{fb}^{0,c}$	0.0709 ± 0.0044	-.58
A_b	0.867 ± 0.035	-1.93
A_c	0.647 ± 0.040	-.52
$\sin^2\theta_{eff}^{LEPT}$	0.23109 ± 0.00029	-1.65
$\sin^2\theta_W$	0.2255 ± 0.0021	1.06
m_W (GeV)	80.41 ± 0.09	.43
m_t (GeV)	173.8 ± 5.0	.54
$1/\alpha$	128.878 ± 0.090	.00

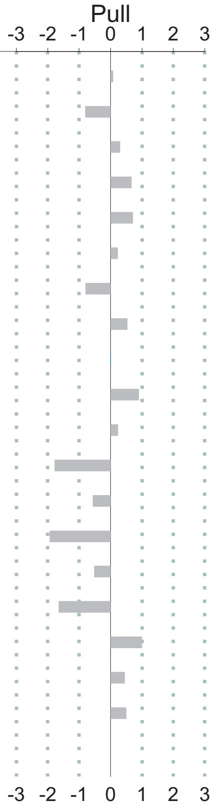

Figure 17: Precision measurements included in the global electroweak fit are shown along with the pulls, defined as the difference between the measurement and the fit value divided by the measurement error. The overall χ^2 of the fit is 15 for 15 degrees of freedom.

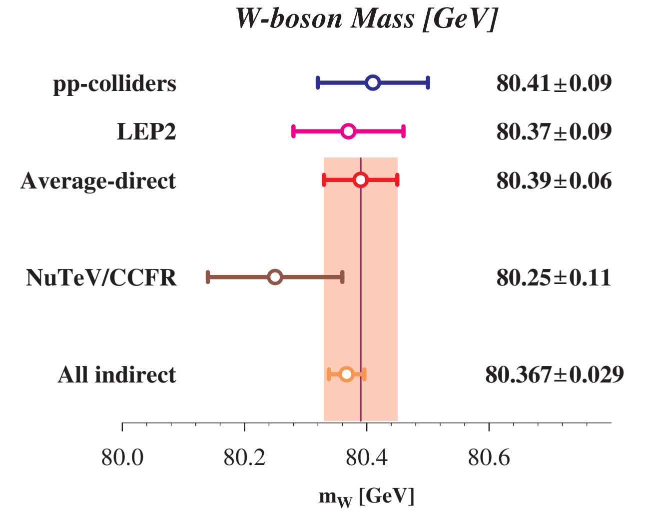

Figure 18: Comparison of direct W mass measurements with indirect determinations. The bottom point is found using all data that is used in the global electroweak fit except the direct W mass measurements.

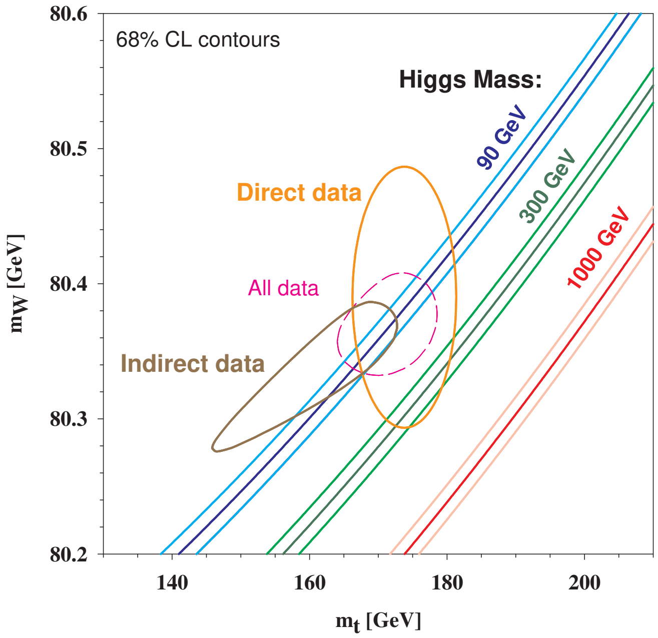

Figure 19: The 68% confidence level contours are shown for the direct and indirect determinations of the top quark and W masses. Also shown, by the dashed contour, is the result using all data, direct and indirect. The diagonal lines show the Standard Model relation for these two quantities, for 3 choices of Higgs mass. The bands for each of these lines show the variation in the Standard Model prediction that arises from the uncertainty in $\alpha(m_Z^2)$, $1/\alpha^{(5)}(m_Z^2) = 128.878 \pm 0.090$.

from the global fit excluding those data in Figure 19. The 68% confidence level contours have significant overlap, and are consistent with Standard Model predictions with a relatively light Higgs mass.

Figure 20 shows the $\Delta\chi^2$ curve of the global electroweak fit as a function of the Higgs mass. The shaded region surrounding the curve is an estimate of the theoretical uncertainty coming from missing higher order terms in the Standard Model calculations. The upper limit on the Higgs mass from the global electroweak fit is,

$$m_{\mathrm{H}} < 262 \ \ \mathrm{GeV} \quad (95\% \ \mathrm{C.L.}) \ ,$$

which includes the theoretical uncertainty but not the direct Higgs search limits.[42]

Figure 20 also shows how the precision of the indirect Higgs mass determination would improve with a more precise estimate of $\alpha(m_Z^2)$.[43]

The indirect Higgs mass determination relies on a large number of precision measurements. The influence that each measurement has on the final result, depends on the precision of the measurement, its sensitivity to the Higgs mass and, of course, the central value of the measurement. Figure 21 shows how the 68% and 95% confidence intervals change as various observables are re-

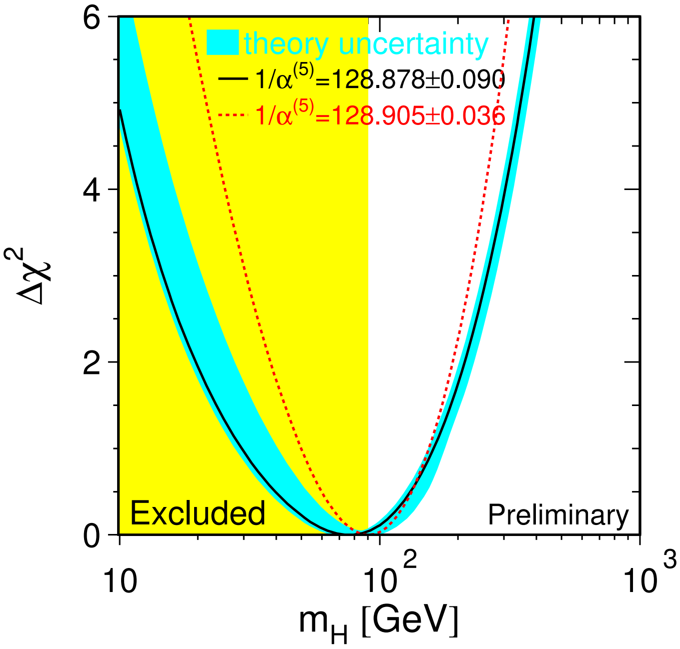

Figure 20: The change in χ^2 of the global electroweak fit as the Higgs mass is varied between 10 and 400 GeV. The band represents an estimate of the uncertainty from missing higher order corrections. The shaded area indicates the excluded region from the direct Higgs searches at LEP. The dashed curve shows the improvement in the indirect determination that is possible with a more precise estimate of $\alpha(m_Z^2)$.

moved. There is a rather large variation in the confidence intervals, however there is no justification to discard any of the measurements, as none of the pulls, shown in Figure 17 are significant.

6 Conclusions

Precision Z^0 measurements at LEP are nearing completion. These results represent a great deal of careful and systematic work. The SLD experiment has requested another data taking run at SLC to further improve the important polarisation measurements.

The LEP II data sample is growing rapidly, and with the year 2000 run now approved, the goal of 500 pb^{-1} of integrated luminosity per experiment appears to be within reach. At the Tevatron, the Run II program is eagerly awaited, with a goal of 2 fb^{-1} to be delivered to each experiment. With these large data samples, the LEP and Tevatron W mass measurements should each achieve precision of about 40 MeV.

The success of the Standard Model to account for measurements with continually increased precision is quite remarkable. In the framework of this model, a scalar Higgs boson is predicted to exist at a mass that is accessible by present or future hadron and lepton colliders. The eventual discovery of the Higgs boson would undoubtably be the greatest triumph of the Standard Model.

Acknowledgements

I owe thanks to a large number of people for their help in preparation of this presentation, including, Bob Clare, Martin Grünewald, and the LEP Electroweak working group, Tom Bolton (NuTeV), Ashutosh Kotwal and Tom Diehl (D0), Eric Lancon and Reisaburo Tanaka (ALEPH), Stephan Wynhoff, Giovanni Passaleva, Nicanor Colino, and Luca Malgeri (L3), Tatsuo Kawamoto, David Strom, Mark Thomson, Michael Kobel, and Gideon Bella (OPAL), Niels Kjaer (DELPHI), Morris Swartz and Tony Johnson (SLD), Fred Harris (BES), and Charles Timmermans (E821).

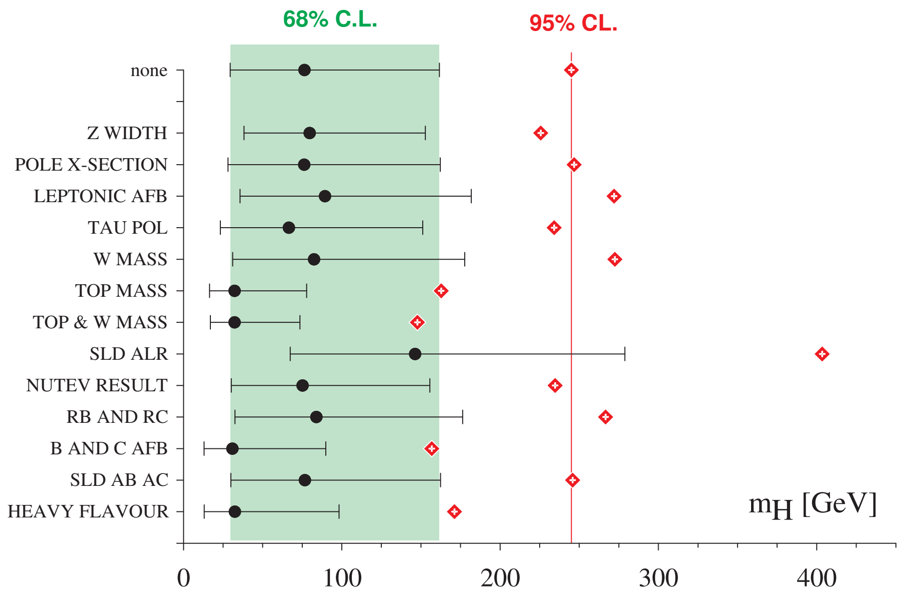

Figure 21: The influence of individual measurements on the indirect determination of the Higgs mass is demonstrated by showing the results when each is removed. The axis on the left shows the particular observable removed, the solid circle and error bar shows the central value and the 68% confidence interval, and the diamonds indicate the 95% confidence interval. The top point is the result with no measurements removed, for reference. The theory uncertainty is not included.

References

1. S. Weinberg, *Phys. Rev. Lett.* **19**, 1264 (1967);
   A. Salam, p. 367 of *Elementary Particle Theory*, ed. N. Svartholm (Almquist and Wiksells, Stockholm, 1969);
   S. L. Glashow, J. Iliopoulos, and L. Maiani, *Phys. Rev.* D **2**, 1285 (1970).
2. R. Assmann, *et al.*, *Calibration of centre-of-mass energues at LEP-1 for precise measurements of Z properties*, CERN-EP/98-40 (March 1998), submitted to European Physical Journal C.
3. B. Bloch-Devaux, *these proceedings*.
4. M. Hildreth, *these proceedings*.
5. ALEPH Collaboration, ALEPH 98-048.
6. M. Swartz, private communication.
7. A. V. Kotwal, *these proceedings*.
8. M. Thomson, *these proceedings*.
9. N. Watson, *these proceedings*.
10. R. Moller, *these proceedings*.
11. P. Derwent, *these proceedings*.
12. H. Przysiezniak, *these proceedings*.
13. G. Passaleva, *these proceedings*.
14. T. Matsushita, *these proceedings*.
15. L. Malgeri, *these proceedings*.
16. V. Obraztsov, *these proceedings*.
17. R. Tanaka, *these proceedings*.
18. H. Phillips, *these proceedings*.
19. T. Diehl, *these proceedings*.
20. M. Grünewald, *these proceedings*.
21. The LEP Electroweak Working Group, R. Clare, *et al.*, *A Combination of Preliminary Electroweak Measurements and Constraints on the Standard Model*, CERN-EP/98 note in preparation.
22. S. Jadach, *et al.*, *Phys. Lett.* B **257**, 173 (1991).
23. M. Skrzypek, *Acta Phys. Pol.* B **23**, 135 (1992).
24. G. Montagna, *et al.*, *Phys. Lett.* B **406**, 243 (1997).
25. B. Ward, *these proceedings*.
26. K. Baird, *these proceedings*.
27. J.C. Brient, *these proceedings*.
28. G. Borisov, *these proceedings*.
29. A.W. Halley, *these proceedings*.
30. S. Fahey, *these proceedings*.
31. The LEP experiments (ALEPH, DELPHI, L3, and OPAL), *Nucl. Inst. Meth.* A **378**, 101 (1996).
32. S. Wynhoff, *these proceedings*.
33. O. Cooke, *these proceedings*.
34. N. Colino, *these proceedings*.
35. M. Kobel, *these proceedings*.
36. T. Bolton, *these proceedings*.
37. A. Hoecker, *these proceedings*.
38. W. Hollik, *these proceedings*.
39. C. Timmermans, *these proceedings*.
40. M. Steinhauser, *Phys. Lett.* B **429**, 158 (1998).
41. S. Edelmann and F. Jegerlehner, *Z. Phys.* C **67**, 585 (1995).
42. P. McNamara, *these proceedings*.
43. M. Davier and A. Höcker, *Phys. Lett.* B **419**, 419 (1998).